


## ORIGINAL ARTICLE

# Structure-function of anticoagulant TIX-5, the inhibitor of factor Xa-mediated FV activation

Anja Maag<sup>1,2</sup>  | Priyanka Sharma<sup>1</sup> | Tim J. Schuijt<sup>3</sup> | Wil F. Kopatz<sup>4</sup> | Daniëlle Kruijswijk<sup>1</sup> | J. Arnoud Marquart<sup>5</sup> | Tom van der Poll<sup>1</sup> | Tilman M. Hackeng<sup>6</sup> | Gerry A. F. Nicolaes<sup>6</sup> | Joost C. M. Meijers<sup>4,5</sup> | Mettine H. A. Bos<sup>2</sup> | Cornelis van 't Veer<sup>1</sup>

<sup>1</sup>Amsterdam UMC, University of Amsterdam, Center for Experimental and Molecular Medicine, Amsterdam Infection and Immunity Institute, Amsterdam, The Netherlands

<sup>2</sup>Division of Thrombosis and Hemostasis, Leiden University Medical Center, Leiden, The Netherlands

<sup>3</sup>Hospital Gelderse Vallei Ede, Clinical Chemistry and Hematology Laboratory, Ede, The Netherlands

<sup>4</sup>Department of Experimental Vascular Medicine, Amsterdam Cardiovascular Sciences, Amsterdam UMC, University of Amsterdam, Amsterdam, The Netherlands

<sup>5</sup>Department of Molecular and Cellular Hemostasis, Sanquin Research, Amsterdam, The Netherlands

<sup>6</sup>Department of Biochemistry, Cardiovascular Research Institute Maastricht (CARIM) Maastricht University, Maastricht, The Netherlands

## Correspondence

Anja Maag, Departement CEMM, Amsterdam UMC, Meibergdreef 9, 1105 AZ Amsterdam, The Netherlands.  
Email: anjamaag@hotmail.de

## Funding information

Trombosestichting Nederland, Grant/Award Number: TSN2015-2

## Abstract

**Background:** The prothrombinase complex consists of factors Xa (FXa) and Va (FVa) on an anionic phospholipid surface and converts prothrombin into thrombin. Both coagulation factors require activation before complex assembly. We recently identified TIX-5, a unique anticoagulant tick protein that specifically inhibits FXa-mediated activation of FV. Because TIX-5 inhibited thrombin generation in blood plasma, it was concluded that FV activation by FXa contributes importantly to coagulation.

**Objective:** We aimed to unravel the structure-function relationships of TIX-5.

**Method:** We used a structure model generated based on homology with the allergen Der F7.

**Results:** Tick inhibitor of factor Xa toward FV was predicted to consist of a single rod formed by several beta sheets wrapped around a central C-terminal alpha helix. By mutagenesis we could show that two hydrophobic loops at one end of the rod mediate the phospholipid binding of TIX-5. On the other end of the rod an FV interaction region was identified on one side, whereas on the other side an EGK sequence was identified that could potentially form a pseudosubstrate of FXa. All three interaction sites were important for the anticoagulant properties of TIX-5 in a tissue factor-initiated thrombin generation assay as well as in the inhibition of FV activation by FXa in a purified system.

**Conclusion:** The structure-function properties of TIX-5 are in perfect agreement with a protein that inhibits the FXa-mediated activation on a phospholipid surface. The present elucidation of the mechanism of action of TIX-5 will aid in deciphering the processes involved in the initiation phase of blood coagulation.

## KEYWORDS

anticoagulant, factor V, factor Xa, Hemorrhage, thrombin

Manuscript handled by: Alan Mast

Final decision: Alan Mast, 05 April 2021

This is an open access article under the terms of the Creative Commons Attribution-NonCommercial-NoDerivs License, which permits use and distribution in any medium, provided the original work is properly cited, the use is non-commercial and no modifications or adaptations are made.

© 2021 The Authors. *Journal of Thrombosis and Haemostasis* published by Wiley Periodicals LLC on behalf of International Society on Thrombosis and Haemostasis.

### Essentials

- The anticoagulant tick protein TIX-5 specifically inhibits factor Xa (FXa) activation of FV.
- Unraveling the structure-function relationship of TIX-5 using a homology based structural model.
- We identified a phospholipid binding, a potential FXa pseudosubstrate and a FV interaction site.
- The results provide a first insight in how TIX-5 inhibits the FXa activation of FV.

## 1 | INTRODUCTION

The blood coagulation cascade is characterized by a series of enzymatic reactions that result in the thrombin-dependent conversion of soluble fibrinogen to insoluble fibrin fibers. The fibrin fibers are pivotal to stabilizing the initial hemostatic platelet plug formed in a blood vessel lesion that prevents bleeding, but also underlies thrombus formation and potential subsequent ischemia associated with a myriad of pathophysiological processes.<sup>1</sup> Thrombin generation proceeds by the successive activation of various coagulation factors, either by the tissue factor (TF)-dependent extrinsic, or factor XII (FXII)-dependent intrinsic pathway.<sup>2,3</sup> Both pathways culminate in the generation of activated factor X (FXa), with the latter being capable of proteolytic activation of the zymogen prothrombin (FII) into the serine protease thrombin (FIIa). Because FXa is an inefficient enzyme by itself, interaction with its cofactor activated factor V (FVa) on a negatively charged phospholipid layer in the presence of calcium ions to form the prothrombinase complex<sup>4</sup> allows for the efficient and physiologically relevant conversion of prothrombin to thrombin. The cofactor FVa is generated following cleavage at Arg708, Arg1018, and Arg1545 to remove the central B-domain that separates the heavy (a.a. 1–708) and light (a.a. 1546–2145) chains of the procofactor FV. Structurally, the central B-domain appears to cover the FXa binding site of FV by cooperation of acidic (a.a. 1493–1537) and basic (a.a. 963–1008) autoinhibitory sequences guarding the procofactor state of FV.<sup>5</sup> Although both FXa and thrombin are known to be capable of activating purified FV, trace amounts of thrombin formed by FXa alone during the initiation of coagulation have long been recognized as the primary activator of FV.<sup>6–10</sup> However, we recently challenged this paradigm and demonstrated that FXa-dependent activation of FV is a crucial event in the initiation of blood coagulation.<sup>11</sup>

To demonstrate the essential role of FXa in FV activation, we made use of an anticoagulant protein from the saliva of the *Ixodes scapularis* tick known as tick inhibitor of factor Xa toward FV (TIX-5).<sup>11,12</sup> TIX-5 was shown to effectively postpone coagulation by specifically inhibiting FXa-mediated FV activation in the early phase of coagulation during which thrombin-mediated FV activation is restrained by fibrinogen and inhibitors.<sup>11</sup> Although the precise molecular mechanism of TIX-5 inhibition is thus far unknown, this process requires interaction of TIX-5 with the FV B domain.<sup>11</sup> In addition, TIX-5 was found to bind to phospholipids,<sup>11</sup> which are required for FXa-mediated activation of FV.

The importance of FXa-mediated FV activation in plasma appeared dependent on the presence of TF pathway inhibitor  $\alpha$

(TFPI $\alpha$ ) and fibrinogen.<sup>11</sup> Fibrinogen, which is also known as anti-thrombin-I, may bind and occupy thrombin. In this way, fibrinogen restrains thrombin-mediated FV activation and may therefore increase the contribution of FXa-mediated activation of FV to thrombin generation.<sup>13</sup> With regard to the involvement of TFPI $\alpha$ , it inhibits prothrombinase formation by interacting with its basic C-terminal region to intermediate cleaved forms of FV(a).<sup>14,15</sup> Once formed in larger amounts, thrombin will remove the central B-domain of FV by cleavage at Arg709 and Arg1545, including the acidic region TFPI $\alpha$ -binding site on partially activated FV(a).

Here, we characterized the structure-function relationships of TIX-5 to gain insight in its mechanism of action. By generating a homology-based three-dimensional model of TIX-5, regions of interest were identified and targeted for mutagenesis. TIX-5 variants comprising specific modifications at anticipated functional regions were expressed in *Drosophila melanogaster* cells and purified. Our results indicate that the TIX-5 structure is hallmarked by a potential FXa pseudosubstrate cleavage site, an FV-binding site, and two hydrophobic loops that mediate phospholipid binding. All functional regions were shown to be of importance for the anticoagulant activity of TIX-5. These characteristics of TIX-5 fit the functional profile of an inhibitor of phospholipid-dependent FV activation by FXa.

## 2 | METHODS

### 2.1 | Structural modeling

The amino acid sequence of TIX-5 (NCBI AEE89467, UniProt F6KSY2), as reported by Schuijt et al.,<sup>12</sup> was subjected to homology-based structural modeling using the web-based Phyre2 software.<sup>16</sup> Phyre2 identified the Der F7 dust mite allergen (PDB ID 3UV1) from *Dermatophagoides farinae* as the best homologue to generate a homology-based predicted structure of TIX-5. Protein interactive sites on the model structure of TIX-5 were predicted with the aid of the ICM pro software (Molsoft, San Diego, CA).

### 2.2 | TIX-5 protein expression and purification

Wild-type (WT) TIX-5 and TIX-5 variants were expressed in S2 insect cells as described<sup>11</sup> using the pMT/Bip/V5-HisA vector

(Invitrogen, Carlsbad, CA). Point mutations in the coding sequence of TIX-5 were inserted by site-directed mutagenesis (QuikChangeII, Agilent Technologies, Palo Alto, CA) for the different variants using appropriate primers (Table S1); constructs were validated by DNA sequencing. S2 *Drosophila melanogaster* cells were stably transfected with the plasmids encoding for TIX-5 and pCOBlast by calcium chloride transfection and selection with blasticidin (25 µg/ml). For protein expression, *Drosophila* S2 cells were grown at room temperature for 3 days in a spinner flask in serum free medium. Protein expression was induced by 500 µM copper sulfate for 4 days. The cells were harvested by centrifugation at 1000g for 15 min and the supernatant was filtered over a 0.22-µm bottle top filter (Millipore, Burlington, MA). TIX-5 variants were purified from the supernatant by Ni-NTA chromatography (Thermo Fisher Scientific, Waltham, MA) in 10 and 20 mM imidazole, 50 mM NaH<sub>2</sub>PO<sub>4</sub>, 300 mM NaCl, pH 8.0, and eluted from the resin with 250 mM imidazole, 50 mM NaH<sub>2</sub>PO<sub>4</sub>, 300 mM NaCl, pH 8.0. The TIX-5 containing fractions were diluted with MQ water to 100 mM NaCl and cleared over DEAE sepharose (Millipore) equilibrated with 50 mM Tris, 150 mM NaCl, pH 7.4. The fractions containing TIX-5 were loaded onto SP sepharose (Millipore) that was equilibrated in 25 mM MES, 100 mM NaCl, pH 6.5, washed with the same buffer, and eluted in the same buffer with 1 M NaCl. The fractions containing TIX-5 were concentrated with an Amicon ultra centrifugal filter unit (10 kDa MWCO, Millipore) and washed with phosphate buffered saline (PBS). Next, the concentrate was subjected to size exclusion chromatography (S200 26/600) (GE Healthcare, Uppsala, Sweden) in PBS to eliminate trace contaminants, followed by concentration as described previously. The protein concentration was determined by measuring the absorbance at 280 nm (molar absorption coefficient  $\epsilon = 0.4$ ). Aliquots were flash frozen in liquid nitrogen and stored at -80°C. Purity was assessed by sodium dodecyl sulphate–polyacrylamide gel electrophoresis (SDS-PAGE) on 12% polyacrylamide gels and Coomassie staining. To assess protein backbone molecular weight of the TIX-5 and variant proteins were deglycosylated with PNGase F (New England Biolabs) overnight in PBS containing 0.75% Triton X-100 and evaluated by SDS-PAGE on 15% gels.

### 2.3 | Human plasma and coagulation factors

Factor Xa was obtained from Enzyme Research Laboratories (South Bend, IN). Recombinant human FV-B1033 and FV-B104, respectively, used for FV activation and FV binding experiments were kindly provided by Dr. Rodney Camire (Division of Hematology, Department of Pediatrics, Perelman School of Medicine, University of Pennsylvania). Normal human platelet poor pooled citrated plasma was kindly provided by the Department of Experimental Vascular Medicine, Amsterdam University Medical Centers (Academic Medical Center, the Netherlands).

### 2.4 | Calibrated automated thrombography

Thrombin generation was performed in platelet poor plasma with a Fluoroskan Ascent microtiter plate-reading fluorometer (Thermo Labsystems, Philadelphia, PA) and Thrombinoscope software (Thrombinoscope B.V., Maastricht, The Netherlands) according to the manufacturer's instructions and Hemker et al.<sup>17</sup> Before the analysis, pooled normal human plasma was thawed for 15 min at 37°C. In an Immulon 2HB microtiter 96-well plate (Thermo Fisher Scientific), 80 µl of plasma was added to 20 µl of PPP reagent (Thrombinoscope B.V.), resulting in a final concentration of 5 pM relipidated TF. Additionally, 10 µl TIX-5 (4 µM final concentration) or vehicle PBS was added to the reaction. Thrombin calibrator (Thrombinoscope B.V.) was used as calibration standard. After 10 min of incubation at 37°C, thrombin generation was initiated by automated dispensing of 20 µl of the fluorogenic substrate in calcium buffer (FluCa Kit, Thrombinoscope B.V.). The fluorescent signal was detected at 390 nm (excitation filter) and 460 nm (emission filter) for 60 min in 20-s intervals. The following parameters were calculated by the Thrombinoscope software: lagtime in min, time to peak (ttpeak) in min, endogenous thrombin potential (ETP) in nM\*min, peak thrombin concentration in nM, and velocity index in nM/min.

### 2.5 | Surface plasmon resonance analysis

The binding of TIX-5 to phospholipids was analyzed with a BIACORE 3000 (GE Healthcare). Before immobilization of the phospholipids, a research grade L1 chip (GE Healthcare) was equilibrated with 10 mM HEPES, 150 mM NaCl, pH 7.4, and cleaned with 40 mM B-octyl glycoside. Phospholipid vesicles consisting of phosphatidylcholine, phosphatidylserine, and phosphatidylethanolamine (60%:20%:20%, respectively) in flow buffer were immobilized on the L1 chip up to 5500 RU, and the channel was stabilized by 100 mM NaOH and 5 mM EDTA. The TIX-5 variants were injected at 100 nM in 10 mM HEPES, 150 mM NaCl, pH 7.4. The curves were processed by BiaEvaluation 4.1 software (GE Healthcare).

### 2.6 | TIX-5 binding to immobilized FV

The binding of TIX-5 to FV-B104<sup>5</sup> was determined by solid-phase binding analysis. Briefly, 3 µg/ml of FV was adsorbed onto high-binding microtiter wells (Thermo Fisher Scientific) in PBS with 1 mM CaCl<sub>2</sub> for 120 min at room temperature and blocked with 1% bovine serum albumin (BSA) in 20 mM HEPES, 150 mM NaCl, 2 mM CaCl<sub>2</sub>, pH 7.4. Subsequently 2.5 µg/ml TIX-5 variant diluted in 20 mM HEPES, 150 mM NaCl, 2 mM CaCl<sub>2</sub>, 1% BSA, pH 7.4, was incubated with the adsorbed FV for 60 min at room temperature. Upon washing with 20 mM HEPES, 150 mM NaCl, 2 mM CaCl<sub>2</sub>, pH 7.4, bound TIX-5 was detected using horseradish peroxidase-labeled anti-V5 antibody (Life Technologies, Rockville, MD) by 3,3',5,5'-tetramethylbenzidine

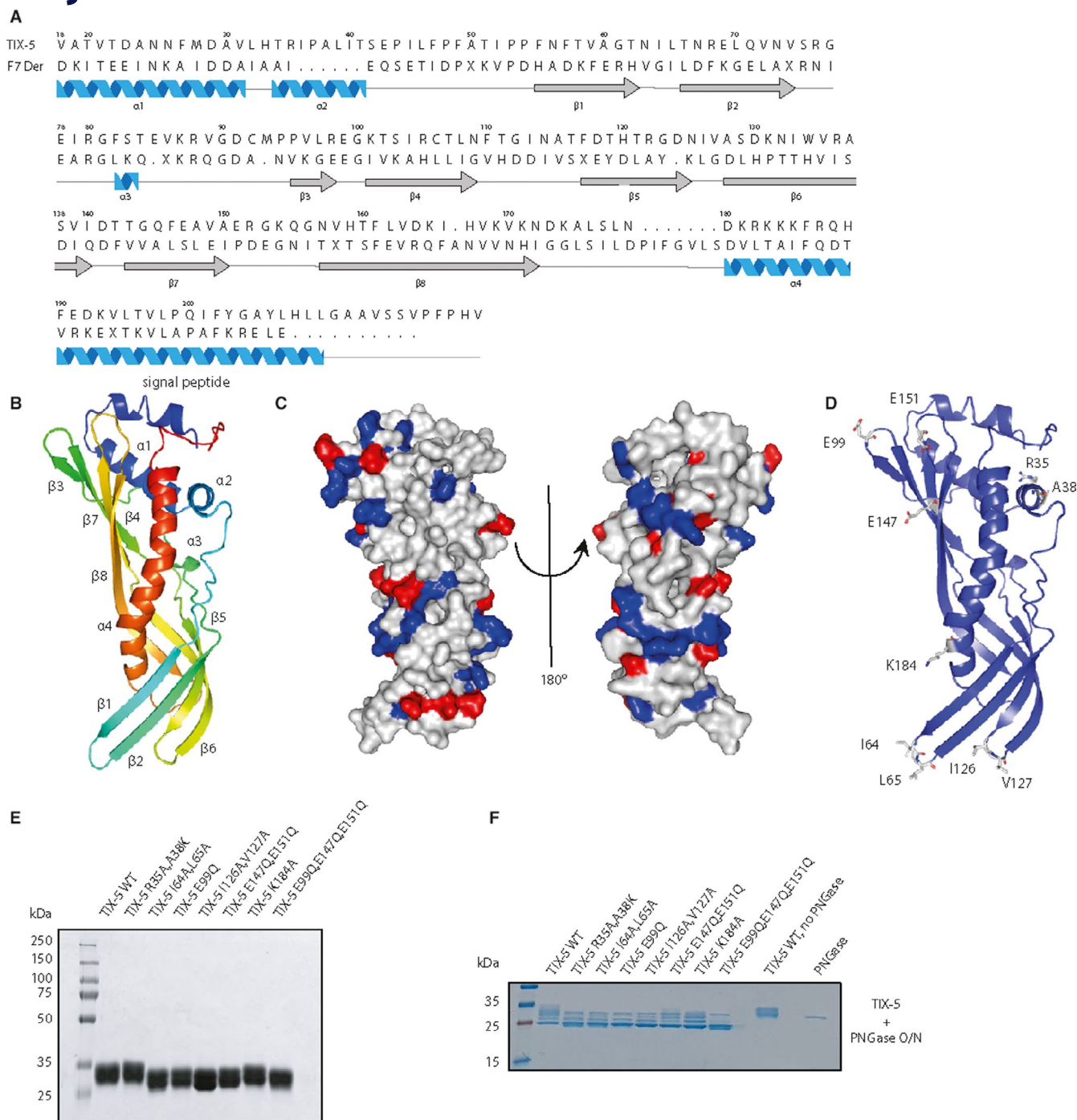


**FIGURE 1** Homology modeling of the TIX-5 protein structure and TIX-5 mutagenesis. (A) The mature amino acid sequence of TIX-5 was aligned with that of Der F7 using Jalview software.<sup>23</sup> Boundaries of the secondary structure of TIX-5 as determined by Phyre2 are indicated below the sequences, with  $\alpha$ -helices in blue and  $\beta$ -sheets in gray. (B) Ribbon diagram of TIX-5, with the N-terminus indicated in red and the C-terminus in blue. The two-helix region at the N-terminus is labeled as the “signal peptide.” (C) Two different views of the A surface charge diagram of TIX-5 displaying the positively charged residues in blue and negatively charged residues in red. The ‘standard view’ of TIX-5 is shown on the left (see panels B and D) and rotated at 180° on the right. (D) Ribbon diagram of TIX-5 including residues that were predicted to be pivotal for the anticoagulant activity. The images in panels B–D were generated using Pymol software.<sup>24</sup> (E) SDS-PAGE analysis of purified recombinant TIX-5 variants (5  $\mu$ g/lane) and visualized by staining with Coomassie Brilliant Blue. WT TIX-5 and mutants were purified to the same extent. The apparent molecular weights of the standards are indicated. (F) SDS-PAGE analysis of purified recombinant TIX-5 variants (3.5  $\mu$ g/lane) incubated with PNGase overnight (O/N) and visualized by staining with Coomassie Brilliant Blue. The molecular weights of the standards are indicated. SDS-PAGE, sodium dodecyl sulphate–polyacrylamide gel electrophoresis; TIX, tick inhibitor of factor Xa; WT, wild-type

staining. Nonspecific binding of TIX-5 variant was determined in 1% BSA-blocked wells and subtracted from the binding observed in FV-coated wells.

2.7 | FV activation by FXa

The biochemical activation of FV-B1033 by FXa was assessed at 37°C in 20 mM HEPES, 137 mM NaCl, 3 mM CaCl<sub>2</sub>, 0.3% BSA, pH 7.4, containing 4 μM phospholipid (MP reagent, Thromboscope B.V.), 10 nM FV-1033, 6 μM TIX-5 variant or PBS as vehicle control. The reaction was started by the addition of 1 nM FXa. Samples were taken and added to four volumes of 1.25-fold concentrated SDS-PAGE loading buffer. After heating for 5 min at 95°C, proteins were separated by SDS-PAGE on 7.5% polyacrylamide gels and transferred to polyvinylidene fluoride membranes for western blotting with anti FV heavy chain antibody AHV-5146 (Haematologic Technologies, Essex Junction, VT) to visualize FV activation.

2.8 | Potential proteolysis of TIX-5 by FXa

WT TIX-5 and E99Q TIX-5 (160 μg/ml) were incubated for 1 and 2 h with 50 nM FXa to assess possible cleavage of TIX-5 by FXa. Also, FV (20 nM) was added to promote proteolysis. After heating for 5 min at 95°C, proteins were separated by SDS-PAGE under reducing conditions on 15% polyacrylamide gels and transferred to polyvinylidene fluoride membranes for western blotting with anti V5 antibody (Invitrogen) to visualize potential proteolysis of TIX-5 by FXa.

2.9 | Statistical analysis

Data were analyzed using GraphPad Prism, version 5.01 (GraphPad Software San Diego, CA). Statistical analysis was performed using the Mann-Whitney *U*-test; *p* values <.05 were considered statistically significant.

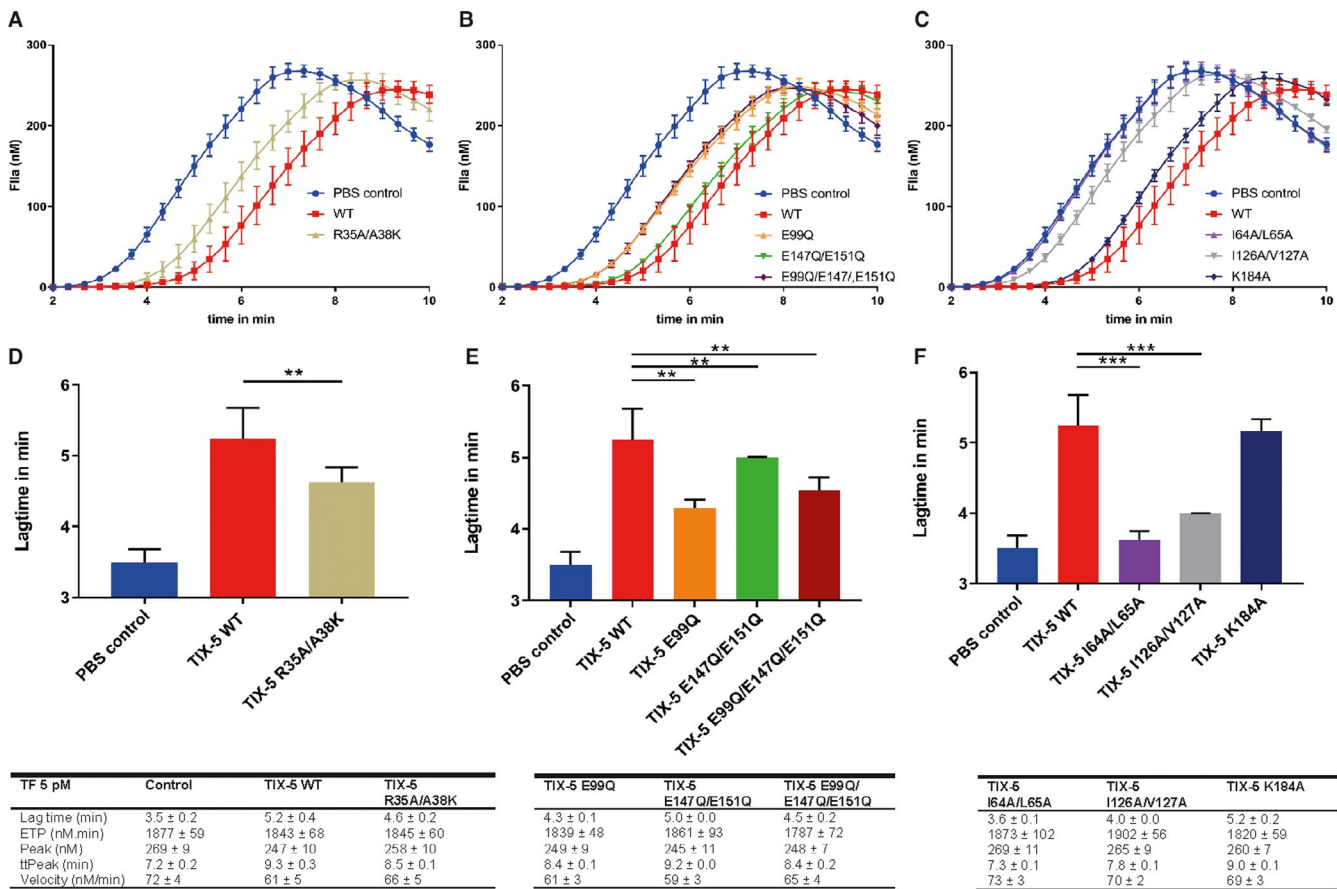


**FIGURE 2** Effect of TIX-5 variants on TF-initiated thrombin generation. Thrombin generation was initiated with 5 pM TF in pooled normal human plasma (NHP) in the absence or presence of 4 μM TIX-5. (A-C) Thrombograms representing NHP in the absence of TIX-5 (control, blue), WT TIX-5 (red), TIX-5 R35A/A38 K (beige), TIX-5 E99Q (orange), TIX-5 E147Q/E151Q (green), TIX-5 E99Q/E147Q/E151Q (dark red), TIX-5 I64A/L65A (purple), TIX-5 I126A/V127A (gray), and TIX-5 K184A (dark blue). (D-E) Lagtimes of the thrombograms in the absence or presence of TIX-5 are shown. The data represent means ± SD of eight replicates. \**p* < .05, \*\**p* < .01, \*\*\**p* < .005. SD, standard deviation; TF, tissue factor; TIX, tick inhibitor of factor Xa



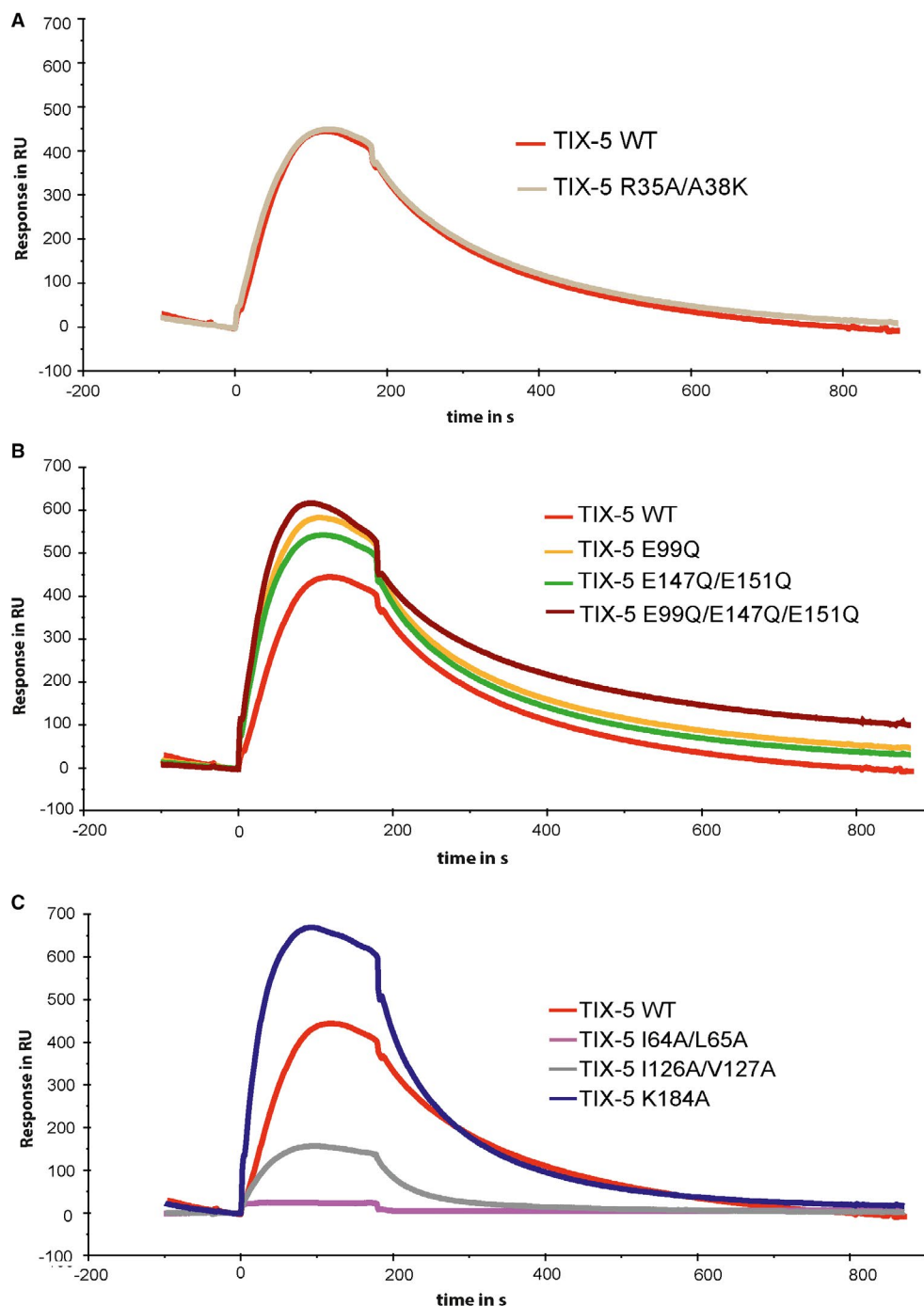


**FIGURE 3** Phospholipid interaction of TIX-5 variants. (A–C) Phospholipids (phosphatidylcholine:phosphatidylserine:phosphatidylethanolamine, 60%:20%:20%) were immobilized on an L1 chip, and 100 nM TIX-5 was passed over the immobilized phospholipids for 200 s, upon which the TIX-5-containing buffer was replaced by buffer only. The binding is indicated in response units (RU), and the TIX-5 variants assessed are WT TIX-5 (red), TIX-5 R35A/A38 K (beige), TIX-5 E99Q (orange), TIX-5 E147Q/E151Q (green), TIX-5 E99Q/E147Q/E151Q (dark red) TIX-5 I64A/L65A (purple), TIX-5 I126A/V127A (gray), and TIX-5 K184A (dark blue). The data are representative of two individual experiments. TIX, tick inhibitor of factor Xa

### 3 | RESULTS

#### 3.1 | Prediction of functional regions in TIX-5 using homology modeling

The three-dimensional protein structure of TIX-5 was computationally predicted through homology modeling using the protein Der F7

(PDB ID 3UV1), a dust mite allergen from *Dermatophagoides farina*, as structural template. Although the degree of sequence homology between TIX-5 and Der F7 was only 14% (Figure 1A), 82% of the TIX-5 structure was covered with a confidence of 99.7%. In the proposed protein structure, TIX-5 contains eight beta strands that are arranged to form four anti-parallel beta sheets that wrap around the long fourth alpha helix (Figure 1B). Furthermore, TIX-5 was predicted

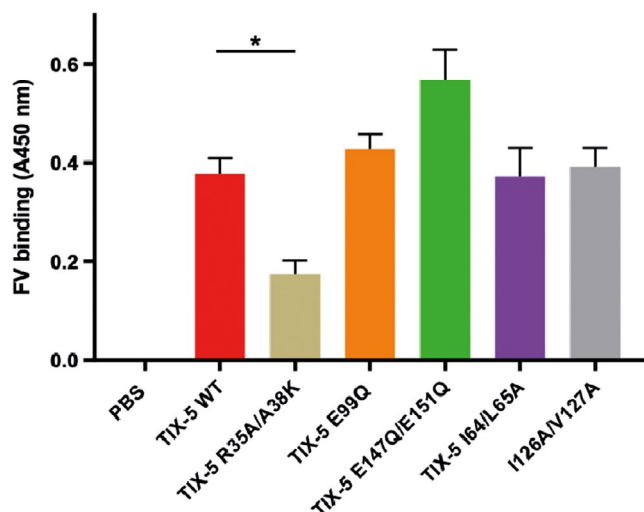


**FIGURE 4** Tick inhibitor of factor Xa (TIX) toward FV variant binding to immobilized FV. TIX-5 variants were incubated with immobilized FV-B104, and associated TIX-5 was assessed. The TIX-5 variants assessed are WT TIX-5 (red), TIX-5 R35A/A38 K (beige), TIX-5 E99Q (orange), TIX-5 E147Q/E151Q (green), TIX-5 E99Q/E147Q/E151Q (dark red), TIX-5 I64A/L65A (purple), TIX-5 I126A/V127A (gray). The data are presented as percentages of the binding of WT TIX-5 and represent means  $\pm$  SD of four individual replicates. \* $p < .05$ . FV, factor V; SD, standard deviation; WT, wild-type

to contain two hydrophobic loops between beta sheets 1/2 and beta sheets 5/6, depicted in Figure 1B at the bottom of the structure. Residues I64/L65 and I126/V127 that form these hydrophobic loops (Figure 1D) could potentially provide phospholipid-interactive regions similar to the hydrophobic loops in the C1 and C2 domains of FV.<sup>18</sup> In addition, the TIX-5 structure indicates the presence of a negatively charged surface-exposed region that includes E99, E147, and E151 (Figure 1D). This region may play a role in the anticoagulant activity of TIX-5 because we have previously demonstrated that the basic B-domain region of FV is involved in the FV-TIX-5 interaction.<sup>11</sup> Furthermore, E99 is interesting because it is part of an extended loop with the sequence EGK (Figure 1A), which resembles EGR, a preferred substrate sequence of FXa.<sup>19</sup> A potential protein binding site included the surface-encompassing residues R35 and A38 (Figure 1D). Finally, within alpha helix 4 of TIX-5, a series of basic residues including the surface-exposed K184 (Figure 1D) were recognized that could be involved in electrostatic interactions with the acidic FV B-domain region or contribute to phospholipid binding, potentially in cooperation with the hydrophobic loops in case of the latter.

Based on the generated homology model for the protein structure of TIX-5, we performed a mutagenesis study to substitute the previously mentioned residues for residues predicted to disable the local interactive surface, but with lack of effect on the overall structure as confirmed by Phyre 2 modeling (data not shown). The generated TIX-5 mutants are (Table S2): double-mutant R35A/A38 K to alter the predicted protein interactive site, E99Q; double-mutant E147Q/E151Q; and triple-mutant E99Q/E147Q/E151Q, to alter the potential FXa cleavage like motif and

negative charge or both, respectively, double-mutant I64A/L65A and double-mutant I126A/V127A and K184A to alter potential phospholipid-binding sites and/or charge in the case of K184A. In line with the predicted TIX-5 structure, all TIX-5 variants displayed protein expression levels comparable to WT TIX-5 in the insect cell supernatant and purified to homogeneity (Figure 1E). TIX-5 is heterogeneous because of differential glycosylation.<sup>11</sup> WT TIX-5 and variants had identical molecular weight after deglycosylation with PNGase F (Figure 1F).

### 3.2 | TIX-5 variants demonstrate reduced anticoagulant activity in thrombin generation analyses

The purified TIX-5 variants were initially assayed for their anticoagulant activity using calibrated automated thrombography. As previously described,<sup>11</sup> WT TIX-5 inhibits TF-initiated thrombin generation by prolonging the lagtime without affecting overall thrombin generation (Figure 2). The predicted protein binding site mutant TIX-5-R35A/A38 K demonstrated reduced anticoagulant activity hallmarked by a shorter lagtime compared with WT TIX-5 (Figure 2A/D). TIX-5-E99Q, with potential altered electrostatic interactions or FXa engagement displayed markedly reduced anticoagulant activity compared with WT TIX-5 (Figure 2B/E), whereas the anticoagulant activity of TIX-5-E147Q/E151Q did not appear to differ substantially from that of WT TIX-5. The triple-mutant TIX-5-E99Q/E147Q/E151Q showed a loss of anticoagulant activity similar to the single-mutant E99Q, indicating that residue E99 plays an important role in the anticoagulant activity of TIX-5. The TIX-5 hydrophobic loop variants were hallmarked by either a substantial, TIX-5-I126A/V127A, or complete, TIX-5-I64A/L65A, loss of anticoagulant activity (Figure 2C,F). This indicates that the hydrophobic patches I64/L65 and I126/V127 provide cooperative interactions that are of pivotal importance to the anticoagulant activity of the TIX-5 protein. The K184A mutant did not display a significant reduction in anticoagulant function compared with WT TIX-5 (Figure 2C,F). Collectively, these data indicate that most of the targeted substitution of residues that were predicted to be important for the anticoagulant action of TIX-5 resulted in a loss of function. As such, this may point to the functional relevance of these TIX-5 residues.

### 3.3 | Hydrophobic regions are involved in the interaction of TIX-5 with a phospholipid surface

Because the pivotal protein interactions of FV, TIX-5, and FXa occur probably on the phospholipid surface, we next assessed the phospholipid-binding properties of the TIX-5 variants by surface plasmon resonance analysis, as previously described.<sup>11</sup> Binding of TIX-5-R35A/A38 K to immobilized phospholipids revealed a response similar to WT TIX-5 (Figure 3A, Table S3),

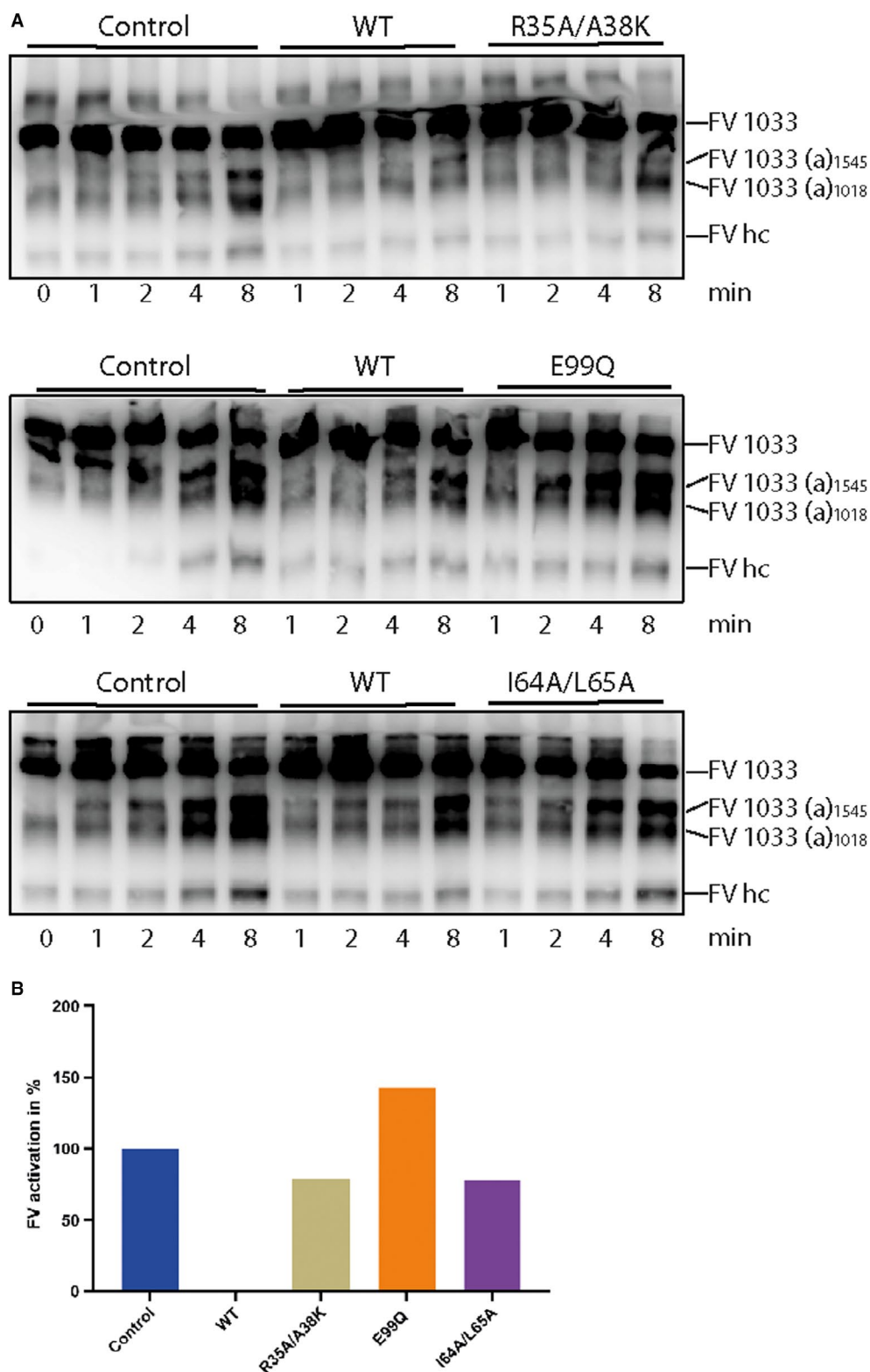


**FIGURE 5** Effect of TIX-5 variants on FV activation by FXa. (A) FV-1033 activation was initiated by 1 nM FXa in the presence of phospholipids and evaluated by western blotting with an anti-FV heavy chain antibody. The FV-1033 activation products following cleavage at Arg709 (the FV heavy chain, FV hc), Arg1018 (FV-1033(a)1018), and Arg1545 (FV-1033(a)1545) and the reaction time points in minutes are indicated. (B) Band intensities of the FV-1033(a) activation products at 4 and 8 min and of the FV heavy chain (HC) at 8 min were quantified and plotted. The mean intensity in the absence of TIX-5 was set at 100% and the mean intensity in the presence of WT TIX-5 at 0%. FV, factor V; FXa, factor Xa; TIX, tick inhibitor of factor Xa



suggesting that residues R35 and A38 are not involved in the TIX-5-lipid interaction. Remarkably, the TIX-5 variants with substitution of the acidic residues E99, E147/E151, or E99Q/E147Q/E151Q all displayed enhanced association for the phospholipid layer compared with WT TIX-5 (Figure 3B, Table S3). Furthermore, substitution of residue K184, which is predicted to be located just above the hydrophobic loops at the bottom of the TIX-5 structure, resulted in an increased association to and increased dissociation from the phospholipid layer relative to WT TIX-5 (Figure 3C, Table S3). Targeting the predicted hydrophobic loops in TIX-5 revealed that no phospholipid binding could be observed of TIX-5-I64A/L65A (Figure 3C), whereas a major reduction in maximum binding was observed for TIX-5-I126A/V127A (Figure 3C). These observations are in line with the predicted role in phospholipid binding of these hydrophobic loops.

### 3.4 | Identification of an FV-interactive region in TIX-5

To gain more insight into the interaction of TIX-5 with FV, we used a solid-phase binding assay to study the interaction of TIX-5 variants with immobilized FV-B104. This FV variant comprises the inhibitory B-domain sequences that likely play a role in the FV-TIX-5 interaction.<sup>5,11</sup> Upon incubation of TIX-5 variants with surface-immobilized FV-B104, specific binding similar to WT TIX-5 was observed for the hydrophobic loop variants TIX-5-I64A/L65A and TIX-5-I126A/V127A and for the TIX-5 variants comprising substitutions at acidic residues E99 and E147/E151 (Figure 4). In contrast, TIX-5-R35A/A38 K displayed significantly reduced FV-B104 binding, suggesting that the alpha helix of which R35 and A38 are part of contributes to the interaction of TIX-5 with FV.

### 3.5 | Identification of functional residues in TIX-5 involved in inhibition of the FXa activation of FV

To further understand the TIX-5 regions and residues that play a role in the inhibition of the FXa-mediated activation of FV, we monitored the proteolytic activation of FV by FXa in the presence of phospholipids, as described previously.<sup>11</sup> In this system, we made use of FV-1033, which also comprises the inhibitory B-domain sequences that have been implicated to contribute to the FV-TIX-5 interaction.<sup>11,20</sup> In line with earlier observations,<sup>11</sup> WT TIX-5 inhibited the activation of FV by FXa/phospholipid, which was indicated by delayed generation of FV(a) intermediates and the FV heavy chain (Figure 5A). Interestingly, TIX-5-R35A/A38 K comprising substitutions in the predicted protein-binding site, the hydrophobic loop variants TIX-5-I64A/L65A, as well as the TIX-5-E99Q mutant, lost the capacity to inhibit FXa-mediated activation

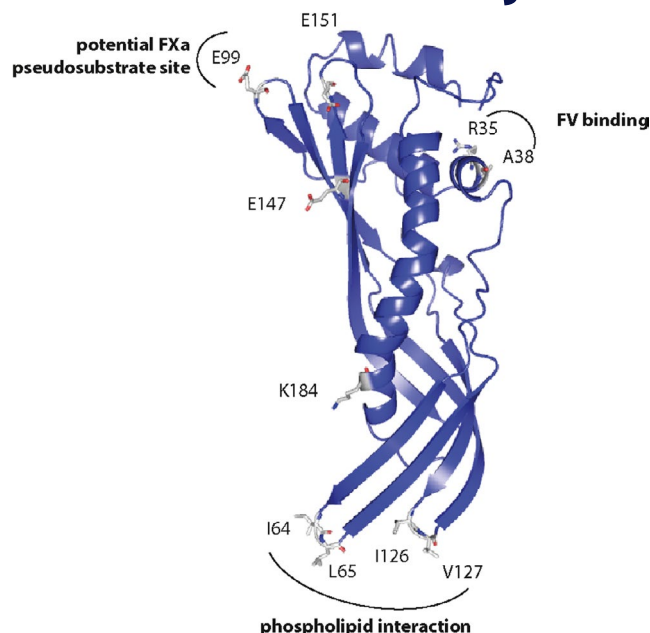


**FIGURE 6** Tick inhibitor of factor Xa (TIX) toward FV model structure and functional regions. Experimentally shown important sites in TIX-5 are the two hydrophobic loops I64/L65 and I126/V127 that interact with phospholipids, the alpha helix with R35/A38 that is involved in FV binding and the loop with E99 containing surface loop comprising a potential FXa pseudosubstrate EGK sequence

of FV (Figure 5A,B). These data indicate that the targeted residues are substantially involved in the inhibition of FXa-mediated FV activation.

## 4 | DISCUSSION

We have previously shown that TIX-5 functions as an anticoagulant that specifically inhibits the activation of FV by FXa.<sup>11</sup> We aimed here to uncover the molecular mechanism that is at the basis of this anticoagulant activity by investigating which residues and/or regions of TIX-5 are pivotal to its function. Straightforward homology modeling of TIX-5 with the webtool Phyre2 rendered an apparently useful three-dimensional model of TIX-5 based on structural homology with the dust mite allergen Der F7 from *Dermatophagoides farina*. Analysis of this predicted structural model led to the identification of several potential functional regions.

Earlier, we had demonstrated that TIX-5 interacts with the FV B-domain, with the basic B-domain region in FV supporting a substantial part of the direct protein-protein interactions.<sup>11</sup> Interestingly, the TIX-5 protein model encompassed negatively charged surface-exposed amino acids, E99, E147, and E151, which were positioned in proximity of each other (Figures 1 and 6) and could facilitate interaction with the FV basic region. However, exchange of these Glu residues for Gln did not impair the TIX-5-FV interaction (Figure 3 and Figure 4). Yet, we found that TIX-5 residue E99 is pivotal for

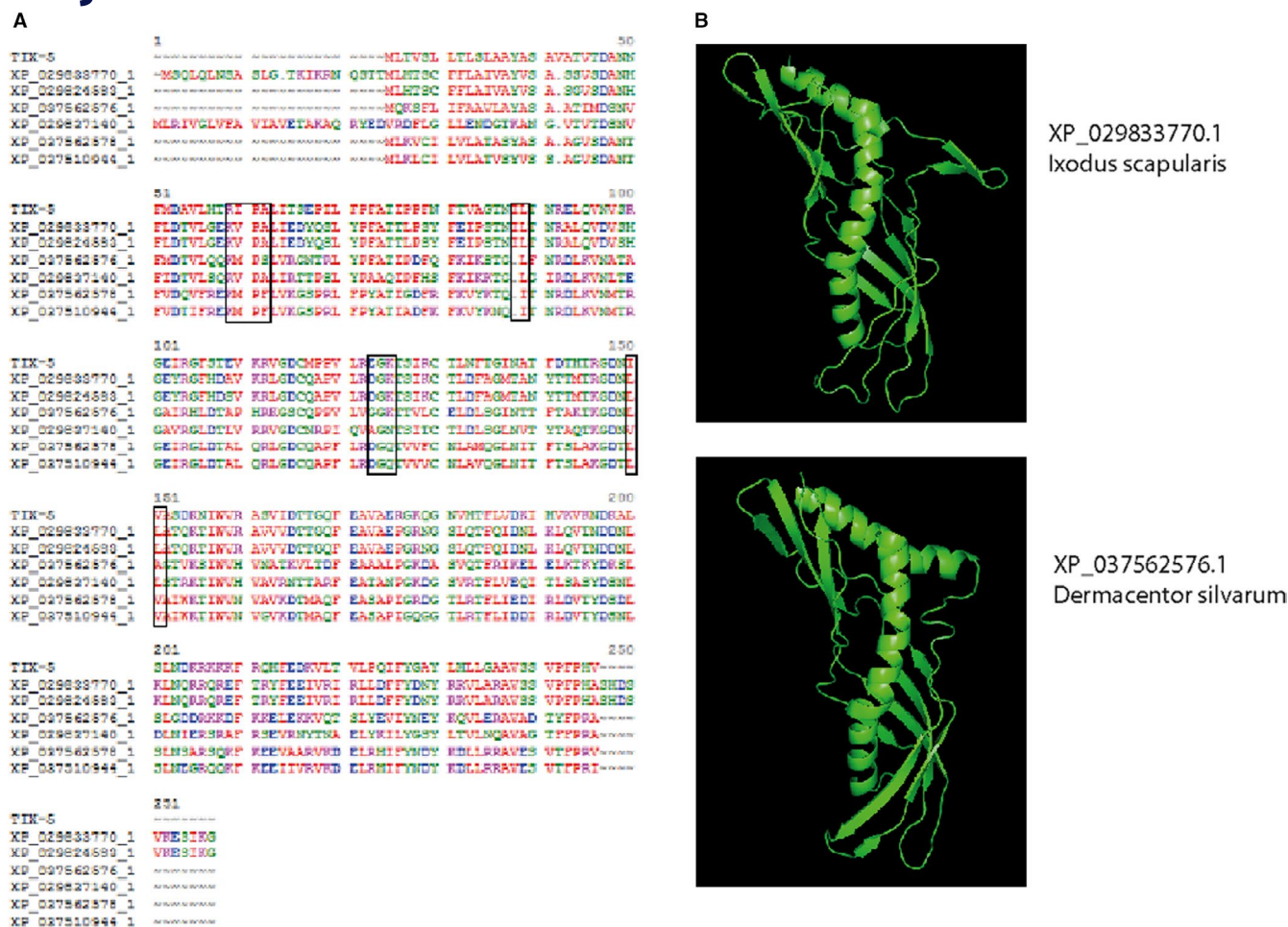


FIGURE 7 Tick inhibitor of factor Xa (TIX) toward FV homology family members. (A) The mature amino acid sequence of TIX-5 was aligned with six nearest homologues, all found in tick species. (B) PyMOL predicted structures of XP\_029833770.1 (*Ixodiscus scapularis*) and XP\_037562576.1 (*Dermacentor silvarum*) are shown as ribbon diagram. The images in panel B were generated using PyMOL software<sup>24</sup>

the anticoagulant function of TIX-5 (Figure 2B,E and Figure 5). As mentioned, we noted that E99 is part of a predicted extended loop E<sup>99</sup>G<sup>100</sup>K<sup>101</sup> (Figure 6) that resembles the EGR substrate sequence of FXa in prothrombin.<sup>19</sup> This may explain why TIX-5 E99Q only displays reduced anticoagulant capacity in functional assays in which TIX-5 potentially acts as a pseudosubstrate for FXa. TIX-5, however, is not cleaved by FXa (Figure S1). In this regard, the P1 arginine for FXa can be substituted by lysine in small fluorogenic substrates.<sup>21</sup> In our prior studies, no TIX-5-dependent inhibition of FXa activity toward a chromogenic substrate or phospholipid-bound prothrombin was observed,<sup>11</sup> indicating a potential specific effect of FV-associated TIX-5 toward FXa that needs further investigation. Conversely, we identified an FV-binding site in the predicted short alpha helix that includes R35 and A38 (Figure 4 and Figure 6) that are important for TIX-5 anticoagulant activity (Figure 2B,D and Figure 5).

Other potential functional TIX-5 regions identified in the predicted TIX-5 structure were two hydrophobic loops comprising residues I64/L65 and I126/V127 (Figure 6), which showed similarities with the hydrophobic loops in the C1 and C2 domains of FV. Interestingly, because the FV C domains facilitate interaction with an

anionic membrane surface,<sup>18</sup> the hydrophobic TIX-5 loops may mediate the previously observed TIX-5-phospholipid binding.<sup>11</sup> Functional analysis of TIX-5 variants I64A/L65A and I126A/V127A showed that loop I64/L65 is crucial for the phospholipid interaction of TIX-5, and I126/V127 strengthening this interaction (Figure 3C). Although both hydrophobic loops were involved in the anticoagulant function of TIX-5 (Figure 2C,F), I64/L65 appeared to contribute most under the conditions used, which is in line with its involvement in phospholipid binding. Furthermore, the I64/L65 loop was also shown to be important for TIX-5 inhibition of FXa-mediated activation of FV (Figure 5). However, neither the I64A/L65A nor the I126A/V127A TIX-5 mutants demonstrated impaired direct binding to FV (Figure 4).

Collectively, our findings show that TIX-5 has specific interaction sites for FV and phospholipids and suggest that it may contain a potential FXa pseudosubstrate site. By identifying these interactions, we have now uncovered the molecular mechanism by which TIX-5, as previously noted,<sup>11</sup> prevents functional low-affinity FXa-FV interactions that drive FXa-mediated FV activation on phospholipid membranes. Why TIX-5 specifically impairs activation of FV by FXa, while not significantly affecting other

functions of FXa and FV, as previously observed,<sup>11</sup> remains unclear at this point. Detailed information on the TIX-5 interactive region(s) in FV that engage with the R35/A38-containing alpha helix and substantiation of the potential pseudosubstrate function of the E<sup>99</sup>GK sequence in TIX-5 would provide further insight. Both of the aforementioned TIX-5 regions appear well oriented for interactions with FV and the FXa active site when TIX-5 is bound to a phospholipid surface (Figure 6).

It is interesting to note that experimental validation of the functional regions identified in TIX-5 based on its three-dimensional homology model confirmed their contribution to the anticoagulant activity of TIX-5. This would imply that the TIX-5 protein structure prediction based on a crystal structure of the dust mite allergen Der F7 is indeed highly accurate, despite a low sequence homology (14%) between the two proteins. Importantly, this is in line with a key principle of structural modeling, which is that protein structure is more conserved in evolution than protein sequence.<sup>16</sup> Der F7 is highly homologous to proteins of the PLUNC family with hydrophobic ligand properties such as the N-terminal domain of bactericidal/permeability-increasing protein that binds phosphatidylcholine.<sup>22</sup> Furthermore, Der F7 binds to bacterial lipopeptide polymyxin B, and is structurally related to juvenile hormone BP, a transporter in butterflies and moths. As such, Der F7 may have immune or hormonal functions, protein inhibitor functions are not reported for Der F7. TIX-5 belongs to a large family of proteins found in ticks with a highly conserved sequence theme (Figure 7A) and a predicted structure similar to TIX-5 (i.e., several  $\beta$ -sheets wrapped around a long central  $\alpha$ -helix) (Figure 7B). The R<sup>35</sup>IPA<sup>38</sup> and E<sup>99</sup>GK<sup>101</sup> sequences in TIX-5, however, are specific for TIX-5 (Figure 7A) that, according to our results, have led to the evolution of TIX-5 as coagulation inhibitor in this protein family.

In conclusion, we generated a working model for the structure of TIX-5 that at first validation performed well in predicting functional parts of TIX-5. Structure-function elucidation of coagulation inhibitors like TIX-5 may aid to get further insight in the initiation phase of blood coagulation.

## ACKNOWLEDGMENTS

This work was financially supported by the Dutch Thrombosis Foundation (TSN2015-2) awarded to CvtV and MHAB. The authors gratefully acknowledge Dr. Rodney Camire (Division of Hematology, Department of Pediatrics, Perelman School of Medicine, University of Pennsylvania) for generously providing FV-B1033 and FV-B104.

## CONFLICT OF INTEREST

None of the authors have a conflict of interest to report.

## AUTHOR CONTRIBUTIONS

Anja Maag: laboratory analysis, interpretation, and drafting of the manuscript. Priyanka Sharma: laboratory analysis. Tim J. Schuijt: revision of the manuscript. Wil F. Kopatz: laboratory analysis. Daniëlle Kruijswijk: laboratory analysis. Arnoud Marquart: laboratory analysis and interpretation. Tom van der Poll: revision of the

manuscript. Tilman M. Hackeng: interpretation of the structure, revision of the manuscript. Gerry A.F. Nicolaes: interpretation of the structure, revision of the manuscript. Joost C.M. Meijers: experimental design, interpretation of laboratory analysis, revision of the manuscript. Mettine H.A. Bos: interpretation and revision of the manuscript. Cornelis van't Veer: experimental design, laboratory analysis, interpretation, drafting and revision of the manuscript.

## ORCID

Anja Maag  <https://orcid.org/0000-0002-9398-9094>

## REFERENCES

1. Blombäck B, Blombäck M. The molecular structure of fibrinogen. *Ann NY Acad Sci*. 1972;202:77-97.
2. Davie EW, Ratnoff OD. Waterfall sequence for intrinsic blood clotting. *Science*. 1964;145:1310-1312.
3. Macfarlane RG. An enzyme cascade in the blood clotting mechanism, and its function as a biochemical amplifier. *Nature*. 1964;202:498-499.
4. Mann KG, Jenny RJ, Krishnaswamy S. Cofactor proteins in the assembly and expression of blood clotting enzyme complexes. *Annu Rev Biochem*. 1988;57:915-956.
5. Bos MHA, Camire RM. A bipartite autoinhibitory region within the B-domain suppresses function in factor V. *J Biol Chem*. 2012;287:26342-26351.
6. Mann KG, Kalafatis M. Factor V: a combination of Dr Jekyll and Mr Hyde. *Blood*. 2003;101:20-30.
7. Orfeo T, Brufatto N, Nesheim ME, Xu H, Butenas S, Mann KG. The factor V activation paradox. *J Biol Chem*. 2004;279:19580-19591.
8. Camire RM, Bos MHA. The molecular basis of factor V and VIII procofactor activation. *J Thromb Haemost JTH*. 2009;7:1951-1961.
9. Hemker HC. The initiation phase—a review of old (clotting-) times. *Thromb Haemost*. 2007;98:20-23.
10. Nicolaes GAF, Dahlbäck B. Factor V and thrombotic disease: description of a Janus-faced protein. *Arterioscler Thromb Vasc Biol*. 2002;22:530-538.
11. Schuijt TJ, Bakhtiari K, Daffre S, et al. Factor Xa activation of factor V is of paramount importance in initiating the coagulation system: lessons from a tick salivary protein. *Circulation*. 2013;128:254-266.
12. Schuijt TJ, Narasimhan S, Daffre S, et al. Identification and characterization of Ixodes scapularis antigens that elicit tick immunity using yeast surface display. *PLoS One*. 2011;6:e15926.
13. Omarova F, Uitte De Willige S, Ariëns RA, Rosing J, Bertina RM, Castoldi E. Inhibition of thrombin-mediated factor V activation contributes to the anticoagulant activity of fibrinogen  $\gamma'$ . *J Thromb Haemost*. 2013;11:1669-1678.
14. Wood JP, Bunce MW, Maroney SA, Tracy PB, Camire RM, Mast AE. Tissue factor pathway inhibitor- $\alpha$  inhibits prothrombinase during the initiation of blood coagulation. *Proc Natl Acad Sci USA*. 2013;110:17838-17843.
15. van Doorn P, Rosing J, Wielders SJ, Hackeng TM, Castoldi E. The C-terminus of tissue factor pathway inhibitor- $\alpha$  inhibits factor V activation by protecting the Arg1545 cleavage site. *J Thromb Haemost JTH*. 2017;15:140-149.
16. Kelley LA, Mezulis S, Yates CM, Wass MN, Sternberg MJ. The Phyre2 web portal for protein modelling, prediction and analysis. *Nat Protoc*. 2015;10:845-858.
17. Hemker HC, Giesen P, AlDieri R, et al. The calibrated automated thrombogram (CAT): a universal routine test for hyper- and hypo-coagulability. *Pathophysiol Haemost Thromb*. 2002;32:249-253.

18. Chaves RC, Dahmane S, Odorico M, Nicolaes GAF, Pellequer J-L. Factor Va alternative conformation reconstruction using atomic force microscopy. *Thromb Haemost*. 2014;112:1167-1173.
19. Brandstetter H, Kühne A, Bode W, et al. X-ray structure of active site-inhibited clotting factor Xa: implications for drug design and substrate recognition. *J Biol Chem*. 1996;271:29988-29992.
20. Zhu H, Toso R, Camire RM. Inhibitory sequences within the B-domain stabilize circulating factor V in an inactive state. *J Biol Chem*. 2007;282:15033-15039.
21. Gosalia DN, Salisbury CM, Maly DJ, Ellman JA, Diamond SL. Profiling serine protease substrate specificity with solution phase fluorogenic peptide microarrays. *Proteomics*. 2005;5:1292-1298.
22. Tan KW, Jobichen C, Ong TC, et al. Crystal structure of Der f 7, a dust mite allergen from dermatophagoides farinae. *PLoS One*. 2012;7:e44850.
23. Waterhouse AM, Procter JB, Martin DMA, Clamp M, Barton GJ. Jalview Version 2—a multiple sequence alignment editor and analysis workbench. *Bioinformatics*. 2009;25:1189-1191.
24. The PyMOL Molecular Graphics System, Version 2.0 Schrödinger, LLC.

## SUPPORTING INFORMATION

Additional supporting information may be found online in the Supporting Information section.

**How to cite this article:** Maag A, Sharma P, Schuijt TJ, et al. Structure-function of anticoagulant TIX-5, the inhibitor of factor Xa-mediated FV activation. *J Thromb Haemost*. 2021;19:1697–1708. <https://doi.org/10.1111/jth.15329>